Appl. Phys. A (2015) 119:61–68
DOI 10.1007/s00339-014-8955-5

Applied Physics A
Materials Science & Processing

High aspect ratio, high-quality microholes in PMMA: a comparison between femtosecond laser drilling in air and in vacuum

Bo Xia · Lan Jiang · Xiaowei Li · Xueliang Yan · Weiwei Zhao · Yongfeng Lu

Received: 10 September 2014 / Accepted: 15 December 2014 / Published online: 23 December 2014

Abstract Microholes, especially high aspect ratio, high-quality microholes with small diameters (<100 μm), have broad applications. However, it is very difficult for traditional drilling methods to obtain deep microholes, especially with aspect ratios of over 50:1. Femtosecond lasers provide a promising solution for efficient drilling of deep microholes with high-precision material removal, reduced recast/microcracks, minimized heat-affected zones, and the absence of plasma-shielding effects. In this work, a comparison study of high aspect ratio, high-quality microholes fabricated in a poly(methyl methacrylate) (PMMA) bulk substrate with the ambient pressure adjusted from 10^5 Pa (air) down to 1 Pa (vacuum) is presented. High aspect ratio (over 100:1) microholes were obtained in a vacuum environment. The contrast between microhole evolution in air and in vacuum was investigated. The results indicate that efficient energy propagation and easy ejection of ablated material/plasma are probably the most important benefits of drilling microholes in vacuum. The dependence of microhole shapes on different fabrication parameters, including pulse energy and ambient pressure, was investigated to quantitatively reveal the underlying mechanisms. The enhanced drilling effect in vacuum was only found in a high pulse energy region ($E_p > 20$ μJ), and it becomes saturated when the ambient pressure was reduced to $\sim 10^2$ Pa at a pulse energy of 50 μJ. Drilling microholes in a vacuum provides a simple and effective way of rapidly fabricating high aspect ratio, high-quality microholes.

B. Xia · L. Jiang · X. Li (✉) · X. Yan · W. Zhao
Laser Micro/Nano-Fabrication Laboratory, School of Mechanical Engineering, Beijing Institute of Technology, Beijing 100081, People's Republic of China
e-mail: lixiaowei@bit.edu.cn

Y. Lu
Department of Electrical Engineering, University of Nebraska-Lincoln, Lincoln, NE 68588-0511, USA

1 Introduction

Drilling of high-quality microholes with small diameters (<100 μm) has recently attracted extensive research due to broad applications in aerospace [1], optical fiber sensors [2], microfluidics [3], biomedical devices [4], and other areas [5]. However, some challenges remain in achieving deep microholes, especially those with an aspect ratio of over 50:1 with ultrahigh power intensities and ultrashort irradiation periods. Femtosecond lasers offer unique advantages, such as high-precision material processing, thereby providing the potential for efficient drilling of deep microholes with reduced recast/microcracks, minimized heat-affected zones, and the absence of plasma-shielding effects.

The benefits of femtosecond laser drilling were first demonstrated by reducing the pulse duration to the femtosecond domain in glass by Verel et al. [6]. Then the drilling process was improved and used in metals by Kamlagea et al. [7, 8] and in polymers by Baudach et al. [9]. A high aspect ratio of over 60:1 without loss of precision was achieved by statically positioning the focus of a femtosecond laser on its front surface with a high processing speed (more than 1.5 μm per pulse) [10]. However, drilling from the front surface of a sample is limited by the ablated material/plasma, which is confined within the narrow channel [11], and the microhole shape formed by previous laser pulses [12]. Machining from the rear surface can eliminate the shape effects of front surface ablation. Straight holes with a 4 μm diameter and more than 200 μm

depth were demonstrated by Li et al. [13]. However, the aspect ratio was limited at about 50:1 because ablated material remained in the narrow channel. At the same time, the processing speed was relatively low (about 0.3 μm/s). Even though the processing speed can be improved to 30 μm/s by applying ultrasonic agitation [14] and 80 μm/s by applying burst-train pulse shaping [15], the aspect ratio can barely be increased as the ablated material obstructs the opening channel. Therefore, elimination of the ablated material/plasma remaining in narrow microholes is a crucial issue if the aspect ratio of the microholes is to be increased by machining from either the front or rear surface.

However, elimination of the ablated material/plasma cannot be achieved just by optimizing laser parameters without a fundamental understanding of the drilling process. In the case of front surface ablation, Esser et al. [11] examined the dynamics of microhole formation and ablation plume physics in time-resolved, side view images recorded with an intensified charge-coupled device (ICCD) camera. Burst-trains with separation times of nanoseconds or longer can be used to improve the aspect ratio. Up to now, several investigations about the drilling process have relied on real-time imaging of the microhole evolution to improve the fundamental understanding of the process, such as Shah et al. [16] and Döring et al. [17]. Besides, the limiting factor of deep microhole drilling is not only the ablation particles which block the microholes or deposit on the side walls, but also the strong nonlinear interaction of femtosecond laser pulses with ambient air. Therefore, it is possible to help the ablation particles escape the deep microholes by creating a low-pressure environment [18]. In addition, with the reduction of air molecules and ablation particles in the vacuum chamber, the air ionization scattering or deflections of the laser beam can be inhibited. So far, the benefits of drilling in vacuum have not been comprehensively investigated in the femtosecond domain, especially for the drilling of high aspect ratio (>60:1) microholes.

In this paper, we present a comparison study on high aspect ratio, high-quality microholes fabricated in a poly(-methyl methacrylate) (PMMA) bulk substrate with the ambient pressure adjusting from 10^5 Pa (air) down to 1 Pa (vacuum). High-quality microholes with a diameter of 25–55 μm and an aspect ratio of over 100:1 were obtained in a vacuum environment. The aspect ratio was approximately two times higher than that in air at the same laser parameters. Using transmission optical microscopy, we investigated the dependence of microhole shape at different fabrication parameters. The enhancement in vacuum occurred when the ambient pressure was reduced from 10^5 to 10^2 Pa and grew a little further at lower pressures. This method provides a simple and effective way to rapidly fabricate high aspect ratio, high-quality microholes.

2 Experimental setup

Figure 1 shows the scheme of the setup used for the experiment. The percussion drilling source was a femtosecond laser system (Spectra-Physics) consisting of a mode-locked Ti:Sapphire oscillator and a regenerative amplifier, producing 50 fs (FWHM) linearly polarized laser pulses at a repetition rate of 1 kHz and a central wavelength of 800 nm. The direction of polarization is parallel to the *y*-axis as shown in Fig. 1. The energy of the laser pulses could be tuned with a group of neutral density (ND) filters. The fs laser beam was statically focused onto the top surface of a polished PMMA bulk sample via a plano-convex lens with a focus length of 100 mm. The sample was placed inside a metallic vacuum chamber with silica glass windows through which the laser beam of 800 nm could pass. The ambient pressure could be regulated from 10^5 Pa (air) to 1 Pa (rough vacuum) by vacuum pump and needle valve. The vacuum chamber was placed on a two-dimensional stage with a load capacity of about 30 kg. The plano-convex lens was fixed on a one-dimensional stage placed outside of the vacuum chamber. In order to detect the spacing between the focus point and the surface of the sample and obtain the images of the shape evolution of the microholes, an illuminator and an imaging system with lenses and a CCD camera were applied on the side view of the sample perpendicular to the direction of the laser propagation. All of the fabricated microholes were characterized by transmission optical microscope or SEM.

3 Results and discussion

3.1 A comparison between microholes drilled in air and in vacuum

Figure 2 shows a comparison of microhole shapes at 5,000 pulses for a pulse energy of 40 μJ drilled in vacuum (1 Pa)

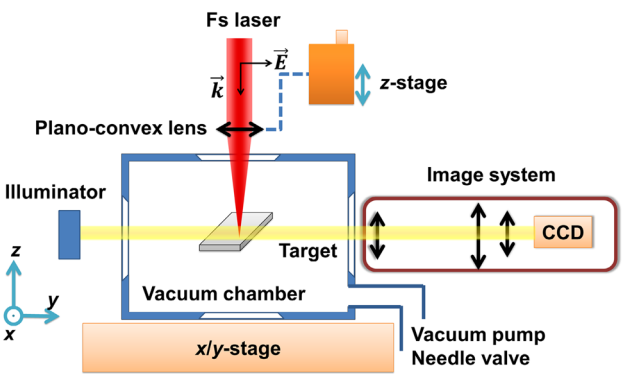

Fig. 1 Schematic illustration of the experiment's setup

and air (10^5 Pa) environments. The microscopy images of the microholes were obtained in *x*/*z*-plane. In a vacuum environment, high aspect ratio (about 109.6) microholes with diameters of about 24 μm and depths of about 2,630 μm were obtained, as shown in Fig. 2a. The microholes appear straight and almost taper free. In contrast, the microholes obtained in an air environment, as seen in Fig. 2f, exhibit diameters of about 24 μm and depths of only about 1,253 μm (an aspect ratio of approximately 50:1). The diameter of the microholes drilled in vacuum (Fig. 2b) is almost the same as that of those drilled in air (Fig. 2g), but the maximum depth of the microholes drilled in vacuum increased by about two times.

In order to compare the quality of the microholes, the magnified transmission optical side view microscopy images of microholes drilled in vacuum and in air are also shown in Fig. 2. For the microholes drilled in a vacuum environment, thin spike and damage can be observed at the entrance (Fig. 2c) and the tips (Fig. 2e) of the microhole. The phenomena are probably caused by the influence of microhole formed previously [12, 19]. The geometry of the air-dielectric boundary which is created by previous laser pulses will strongly affect the laser-field distribution. The different laser waves, including the diffraction waves at the entrance of the channel and reflections waves at the walls of the channel, are overlapping inside the material. At the same time, the distribution of free electron density ionized by modified femtosecond laser is also affected. For the femtosecond laser, certain areas where the ionized free electron density exceeds the critical density will be ablated. Therefore, besides the growth of the microhole depth, the spike structure and optical damage aside the hole are obvious. The high-quality microholes with a well-defined edge are almost taper free for a long distance, as shown in Fig. 2d, and the inside of the microholes is clear, almost without particle deposition. Even at the tips of the microholes, no ablated material is apparent. For microholes drilled in an air environment, a clear wall is observed in the middle of the microholes (Fig. 2i), similar to those drilled in vacuum. However, in contrast to those drilled in vacuum, the damage at the entrance of the microholes drilled in air is much more serious, as shown in Fig. 2h, which is probably due to strong air ionization in the region of the laser focus point. The ablated material/recast drilled in air blocks the microholes and deposits on the side walls of the microholes' tips, as seen in Fig. 2j. The air molecules at a pressure of 10^5 Pa hindered the ablated material from escaping from the microholes, especially from the deep holes. Therefore, creating a low-pressure environment for drilling is an effective method for fabricating high aspect ratio, high-quality microholes.

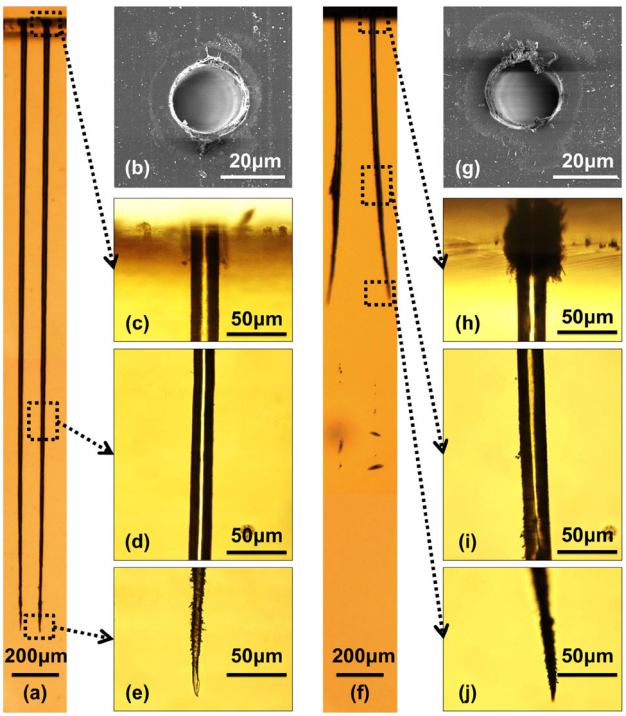

Fig. 2 The comparisons of microhole shapes drilled in vacuum (1 Pa) (**a**) and air (10^5 Pa) (**f**) with 5,000 pulses for a pulse energy of 40 μJ. **c–e**, **h–j** The magnified transmission optical side view microscopy images, refer to (**a**) and (**f**), respectively. **b**, **g** The top view SEM images of microholes drilled in vacuum and air, respectively

Besides, the images of the microholes in *y*/*z*-plane were also checked, which is not shown here. The images of microholes drilled in vacuum are similar in *x*/*z*-plane and *y*/*z*-plane. However, the tip of microhole drilled in air becomes a little bent. The bending tip changes the direction of laser propagation, leading to the ablation bias in one direction. The tip becomes elliptical in a seemingly random direction.

3.2 The contrast of microhole evolution in air and vacuum

a) The propagation of the femtosecond laser

The evolution of the microholes with an increase in the number of pulses (*N*) from 100 to 2,000 was investigated. The energy of the laser pulse was about 30 μJ at a repetition rate of 1 kHz. The microholes became deeper with an increase in the laser pulses, while the diameter of the microholes barely changed, meaning that the femtosecond laser can propagate to the bottom and hardly process the side wall of the microholes. However, comparing the results of drilling in air (10^5 Pa) and in vacuum (1 Pa), the depths of the microholes both grew gradually, but the distinction can clearly be seen in Fig. 3a. In the beginning, the processing speed was maintained constant at the highest value, about 1.23 μm/

pulse in both air and vacuum ($N < 400$). Then the processing speed was kept high in vacuum ($400 < N < 1{,}400$) but was slightly decreased in air ($400 < N < 800$). Finally, the processing speed was subsequently decreased to zero rapidly, and the increase in the depth of the microholes stopped.

In our experiments, as Fig. 3b, c show, the diameters of the microholes were almost the same in air and in vacuum, but the maximum achievable depth of the microholes in vacuum increased by about two times. However, the difference in drilling in air and in vacuum only appeared when the microholes became deeper, as seen in Fig. 3a. The results of the experiment indicate that the higher aspect ratio obtained in vacuum is attributed to the laser drilling deeper inside the microholes. It is probably the different laser propagation mechanism in vacuum and air that leads to achieving high aspect ratio microholes only in vacuum.

In general, there are three mechanisms for laser propagation: (1) the laser propagates to the bottom of a microhole in a straight path; (2) the microhole created by previous laser pulses may act like a waveguide whose side wall reflects subsequent laser pulses to the bottom of the microhole [20]; and (3) the femtosecond filament formed by nonlinear self-focusing and plasma refraction produces a line of weakly ionized plasma channels, which can guide the laser energy to the bottom of the microhole. Hence, in the drilling process, the laser propagation can be influenced by a microhole shape formed previously [19], ablated material/recast deposited on the side walls/tip [21], and laser-induced air breakdown [22]. As drilling began ($N < 400$), the shapes of the microholes looked the same in air and in vacuum, as shown in Fig. 3b, c. Then the processing speed slightly decreased in air ($400 < N < 800$). Therefore, the primary difference in the two environments may rely on the air ionization.

In the air environment (10^5 Pa), the filament is formed when the laser intensity exceeds the ionization threshold. Particularly during deep microhole drilling, the plasma channel affects the stability of beam propagation. The incident laser beam energy partially deposits on random sites, which makes ablation difficult [16]. At the same time, some of the laser energy is lost because of the conical emission [23] (scattering or deflections of the laser caused by air ionization) so that the ablation is stopped without sufficient fluence at the microhole tip. In contrast, in vacuum (1 Pa), the effect of air ionization is reduced because the molecules of air per unit of volume are less. Then the laser can propagate to the bottom of a microhole in a straight path without unnecessary energy loss. The energy of a laser pulse can also propagate to a deep microhole by weakly ionized plasma channels and then ablate the bottom of the microhole. So the final depth of a microhole in a vacuum is deeper than a microhole drilled in air.

b) The ablated material inside the deep microhole

Besides the efficient energy propagation in vacuum, the efficient ejection of ablated material is also a possible explanation for the high aspect ratio in vacuum. In the air, the ablated material/plasma is trapped inside the microholes by the molecules of the atmosphere, especially in the deep microhole drilling process. In comparison, ablated material can be efficiently ejected from a microhole almost without obstacle in vacuum environment.

In order to confirm the ablated material/recast in a microhole drilled in an air environment, we designed an experiment, as seen in Fig. 4. If the ablated material/recast has little effect, the microhole formed in air will be continuously drilled deeper in vacuum because of the efficient energy propagation. First, the microholes were drilled with different pulse numbers in air and vacuum, as seen in Fig. 4a, b, respectively, for a pulse energy of 50 μJ (from left to right, for pulse numbers 200, 500,

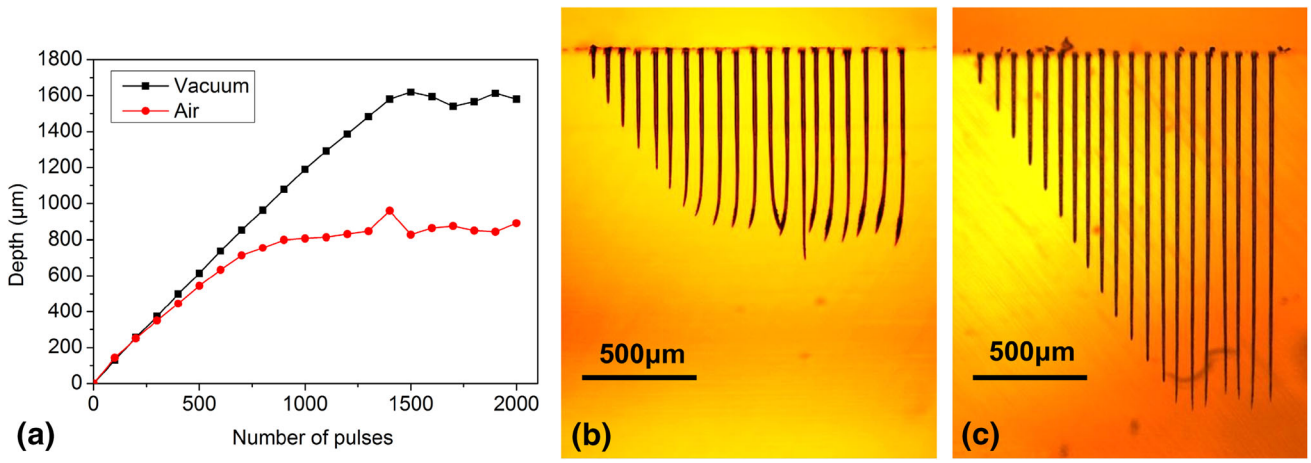

Fig. 3 **a** Development of the microhole depth with the number of pulses increasing from 100 to 2,000 for a pulse energy of 30 μJ. **b**, **c** The development of microhole shapes in air and in vacuum, respectively, corresponding to the data in (**a**)

1,000, and 2,000). Next, we added another 2,000 pulses in vacuum on the microholes formed previously in air (Fig. 4a) as shown in Fig. 4c). Only the shallow microholes could continue to be drilled (in the left of Fig. 4c), and the deep microholes formed in air inhibited the propagation of the laser energy (in the right of Fig. 4c). In order to exclude other factors which may lead to this result, for example, the error of focus spot position caused by stage movement while transferring from air to vacuum, comparative experiments were done in vacuum (Fig. 4b), as shown in Fig. 4d. All of the previously formed microholes could be drilled deeper inside. The results demonstrate that microholes drilled in air have a sharp tip with 200 pulses but can also be reprocessed in vacuum, as shown in Fig. 4c. Moreover, the deep microholes drilled in vacuum with 1,000 pulses also had a sharp tip and could be further processed, as shown in Fig. 4d. Therefore, the tapering microhole shape has little influence on the drilling process, but the little bend at the tip may be the reason that ablation stops as it is misleading for the laser propagation, as seen at the last microhole in Fig. 4c. However, the second microhole in Fig. 4c shows that the ablation almost stopped without bend, perhaps because the tip of the microhole drilled in air became unclear, as shown in Fig. 2j. The results demonstrate that the effect of the ablated material/recast is probably another reason the ablation stops because of the scattering or deflections of the laser beam. It only occurs in the deep microholes in an air environment.

Fig. 4 Microholes drilled in air (**a**) and vacuum (**b**) with different pulse numbers (microholes from left to right are shown for 200, 500, 1,000, 2,000, respectively) for a pulse energy of 50 μJ. **c**, **d** The microholes processed with another 2,000 pulses in vacuum added onto the microholes in (**a**) and (**b**), respectively

c) The bending of the holes at higher depths

Besides the contrast of microhole's depth in air and vacuum, there is another interesting difference between drilling in air and vacuum. Bending of the holes at higher depths is evident at the end of laser drilling process as shown in the Fig. 3b and is almost only occurred in the air environment. While in the vacuum environment, the hole looks straight during the whole drilling process as shown in the Fig. 3c. The phenomena may be attributed to some mechanisms, which disturb the laser propagation process. There are two possible reasons to explain the bending phenomena. One of the possible reasons is that the filament formed in air condition tends to be unstable, and the laser beam energy will be deposited along an orientation deviating from the original direction. Then the direction of the microhole will be changed [22]. The other possible reason is related to the scattering or deflections of the laser beam at the ablation particles, which are trapped inside the laser-drilled channel. Femtosecond laser pulses are then deposited along a bent direction, leading to a change in the direction of the drilling process [17]. In comparison, ionization of air and residue of ablation particles are efficiently reduced in the vacuum condition. The laser propagates to the bottom of hole in a straight path without disturbance. Therefore, straight microholes can be obtained in vacuum.

3.3 The dependence of microhole shape on the different fabrication parameters

a) Effect of the laser pulse energy

To clarify the range of laser pulse energy which makes drilling in vacuum advantageous, we quantitatively analyzed the variation of the final hole depth with pulse energy in both air (10^5 Pa) and vacuum (1 Pa) environments. Figure 5a reveals that the advantage of drilling in vacuum is only found in the high-energy region. In the low pulse energy regime, for

$E_p < 20$ μJ under our experiment's conditions, both the microholes drilled in air and in vacuum had similar depths. Only shallow microholes could be obtained when the laser energy was lower than 10 μJ. In the high pulse energy regime ($E_p > 20$ μJ), the advantage of drilling in vacuum became more obvious. The maximum achievable depth in a vacuum environment was over 3–4 times of that in air at a pulse energy of about 200 μJ. Note that the diameter of the microholes drilled in air and in vacuum increased with the pulse energy at nearly the same trends, as shown in Fig. 5b.

Based on the final hole depth and diameter, the variation of the maximum aspect ratio when compared to the pulse energy is shown in Fig. 6. The maximum achievable aspect ratio grew as the laser energy grew and reached the extreme point in air (48:1) and in vacuum (109:1) at the same energy, 40 μJ. When the energy was in the range of 40–80 μJ, the aspect ratio was constant at about 40–50:1 in air and 100–110:1 in vacuum. When the energy was higher (>80 μJ), the aspect ratio rose a little in vacuum due to the deeper microhole formed. In contrast, the aspect ratio decreased slightly in air due to the increased diameter but barely increased depth, as shown in Fig. 5a.

At the region of $E_p < 10$ μJ, the aspect ratio was mainly determined by longitudinal distribution of the laser focus point and the shape of the microhole was influenced by the diffraction of the incoming pulses at the entrance and the reflections at the walls of the microhole [19]. At the region of 10 μJ $< E_p <$ 40 μJ, the guiding effect of the weakly ionized plasma channels produced by nonlinear self-focusing and plasma refraction gradually increased. Therefore, the aspect ratio became higher with larger pulse energy. At the same time, with the increase in pulse energy and microhole depth, the negative effects (obstruction of ablated material caused by air pressure and scattering/deflections of the laser energy by air ionization) in an air environment brought about a large difference between the ablation under vacuum conditions and under ambient air. At the region of $E_p > 40$ μJ, the advantage of the weakly ionized plasma channels was great enough and the aspect ratio barely increased further in vacuum. However, the stronger air ionization and ablated material blocking led to almost no increase in depth in an air environment. Therefore, the aspect ratio decreased slightly when the pulse energy increased. The higher energy area (over 200 μJ) has not been studied here, because the silica glass window of the vacuum chamber becomes opaque with sputtering as the ablated material is ejected in the vacuum environment.

b) Effect of the ambient pressure

In order to clearly understand the requirements for ambient pressure to increase the final depth of a microhole, the ambient pressure was regulated from 1 Pa (rough vacuum) to 10^5 Pa (air) by a needle valve. In our experiment, with the parameters described in Sect. 2, the maximum depth of a microhole was reached with no more than 5,000 pulses both in the air and in the vacuum environments for a pulse energy below 200 μJ. The saturation depth under different ambient pressures, ranging from 10^5 to 1 Pa for a pulse energy of 30 and 50 μJ, was investigated, as shown in Fig. 7. We saw a turning point at an ambient pressure of about 10^3 Pa for a pulse energy of 30 μJ and at 10^2 Pa for a pulse energy of 50 μJ. The maximum depth increased gradually as the ambient pressure decreased and remained approximately constant at lower pressures. For the evaporation and the ejection, the pressure $p(T)$ linked to the ablation temperature needed to overcome the ambient pressure p_w. With the lower ambient pressure, the evaporation and the ejection of ablated material/plasma became more efficient. However, the kinetic energy of ejection and evaporation decreased gradually in the process of drilling. Therefore, as the pulse energy gets higher, the turning point appears at lower pressure because the maximum depth of the microhole becomes deeper.

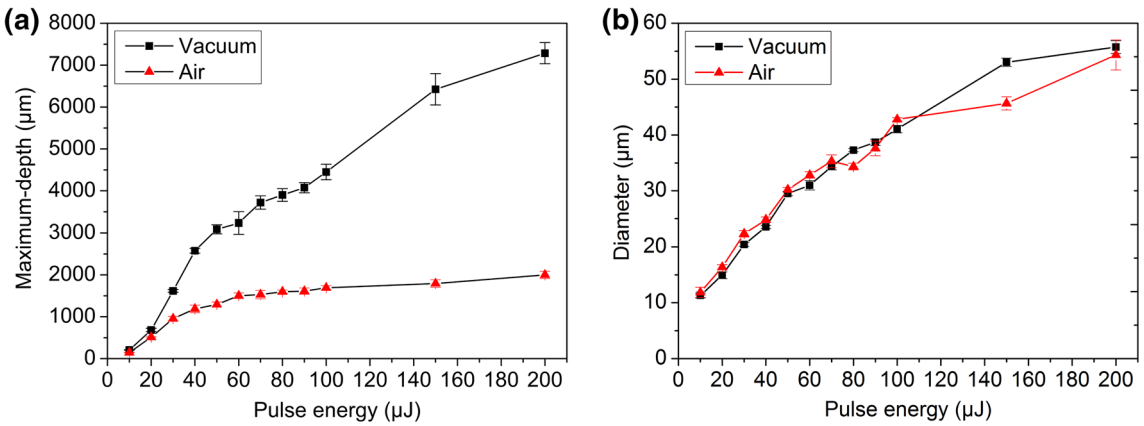

Fig. 5 The variation of the final hole depth (**a**) and diameter (**b**) compared with pulse energy in both air and vacuum environments

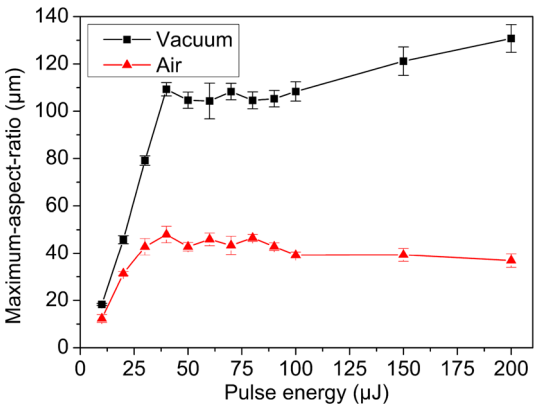

Fig. 6 The variation of the maximum aspect ratio compared with the pulse energy in both air and vacuum environments

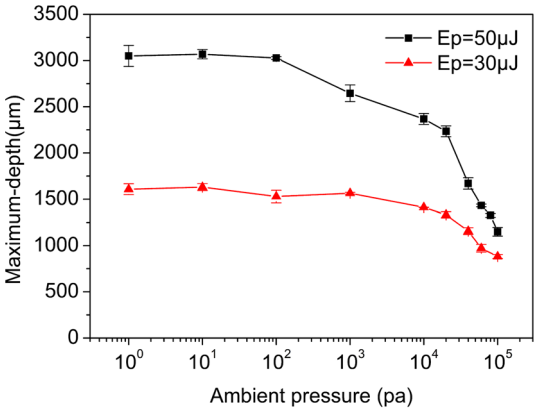

Fig. 7 The maximum depth of microholes drilled with 5,000 pulses for a pulse energy of 30 μJ (*red line* with *triangle points*) and 50 μJ (*black line* with *square points*) at different ambient pressures from 10^5 to 1 Pa

According to the results of the experiment, creating a low-pressure environment for drilling is an effective method for fabricating high aspect ratio, high-quality microholes. However, in this experiment, an ambient pressure lower than 100 Pa was not necessary for energy of 30 and 50 μJ. It is, however, very important in the high-efficiency machining of microholes. The vacuum setup obtained this rough vacuum environment for only a minute in our experiment. It is convenient to replace samples because of rapid switching between air and vacuum.

4 Conclusions

In this paper, a comparison study of high aspect ratio, high-quality microholes fabricated in a PMMA bulk substrate with the ambient pressure adjusted from 10^5 Pa (air) down to 1 Pa (vacuum) was presented. In our experiments, we found that the diameter of the microholes was almost the same in air and in vacuum, but the maximum achievable depths of the microholes in vacuum increased by about two times at the same parameters. High aspect ratio (over 100:1) microholes with a diameter of about 24 μm and a depth of about 2,630 μm were obtained in vacuum. The difference between vacuum and air only occurs deep inside the microhole. On one hand, this is probably attributed to the reduction of the effect of air ionization, enabling the laser to propagate to the bottom of the microhole in a straight path, or to weakly ionized plasma channels without unnecessary energy losses in vacuum. On the other hand, the efficient ejection of ablated material/plasma is also a possible explanation of the deeper microhole drilling in vacuum. Moreover, the dependence of microhole shape on different fabrication parameters (pulse energy and ambient pressure) was investigated. The advantage of drilling in vacuum is only found in the high pulse energy region ($E_p > 20$ μJ). The benefits of this behavior in vacuum occur when the ambient pressure is reduced from $\sim 10^5$ to $\sim 10^2$ Pa and barely changes for lower pressures at a pulse energy of 50 μJ. This provides an effective and simple method for rapidly fabricating high aspect ratio, high-quality microholes.

Acknowledgments This research is supported by the National Basic Research Program of China (973 Program) (Grant 2011CB013000) and National Natural Science Foundation of China (NSFC) (Grants 91323301 and 51305030).

References

1. S. Baheri, S.P.A. Tabrizi, B.A. Jubran, Heat Mass Transfer **44**, 989 (2008)
2. L. Jiang, L.J. Zhao, S.M. Wang, J.P. Yang, Opt. Express **19**, 17591 (2011)
3. Y. Liao, J.X. Song, E. Li, Y. Luo, Y.L. Shen, D.P. Chen, Y. Cheng, Z.Z. Xu, K. Sugioka, K. Midorikawa, Lab Chip **12**, 746 (2012)
4. Z.Z. Fei, X. Hu, H. Choi, S.N. Wang, D. Farson, L.J. Lee, Anal. Chem. **82**, 353 (2010)
5. E.H. Lundgren, A.C. Forsman, M.L. Hoppe, K.A. Moreno, A. Nikroo, Fusion Sci. Technol. **51**, 576 (2007)
6. H. Varel, D. Ashkenasi, A. Rosenfeld, M. Wähmer, E.E.B. Campbell, Appl. Phys. A **65**, 367 (1997)
7. H.K. Tönshoff, C. Momma, A. Ostendorf, S. Nolte, G. Kamlage, J. Laser Appl. **12**, 23 (2000)
8. F. Dausinger, Riken Rev. **50**, 77 (2003)
9. S. Baudach, J. Bonse, J. Krüger, W. Kautek, Appl. Surf. Sci. **154**, 555 (2000)
10. Y. Zhang, R.M. Lowe, E. Harvey, P. Hannadord, A. Endo, Appl. Surf. Sci. **186**, 345 (2002)
11. D. Esser, S. Rezaei, J.Z. Li, P.R. Herman, J. Gottmann, Opt. Express **19**, 25632 (2011)
12. J.R. Vázquez de Aldana, C. Méndez, L. Roso, P. Moreno, J. Phys. D Appl. Phys. **38**, 2764 (2005)
13. Y. Li, K. Itoh, W. Watanabe, K. Yamada, D. Kuroda, J. Nishii, Y.Y. Jiang, Opt. Lett. **26**, 1912 (2001)
14. D.J. Hwang, T.Y. Choi, C.P. Grigoropoulos, Appl. Phys. A **79**, 605 (2004)
15. L. Jiang, P.J. Liu, X.L. Yan, N. Leng, C.C. Xu, H. Xiao, Y.F. Lu, Opt. Lett. **37**, 2781 (2012)

16. L. Shah, O.G. Kosareva, A.A. Koltun, IEEE J. Quantum Elect. **40**, 57 (2004)
17. S. Döring, S. Richter, S. Nolte, A. Tünnermann, Opt. Express **18**, 20395 (2010)
18. S. Döring, S. Richter, F. Heisler, T. Ullsperger, A. Tünnermann, S. Nolte, Appl. Phys. A **112**, 623 (2013)
19. J.R. Vázquez de Aldana, C. Méndez, L. Roso, Opt. Express **14**, 1329 (2006)
20. S. Tao, B.X. Wu, S.T. Lei, J. Appl. Phys. **109**, 123506 (2011)
21. S. Döring, S. Richter, A. Tünnermann, S. Nolte, Proc. SPIE **8247**, 824717 (2013)
22. L. Shah, J. Tawney, M. Richardson, K. Richardson, Appl. Surf. Sci. **183**, 151 (2001)
23. S. Klimentov, P. Pivovarov, N. Fedorov, S. Guizard, F. Dausinger, V. Konov, Appl. Phys. B **105**, 495 (2011)